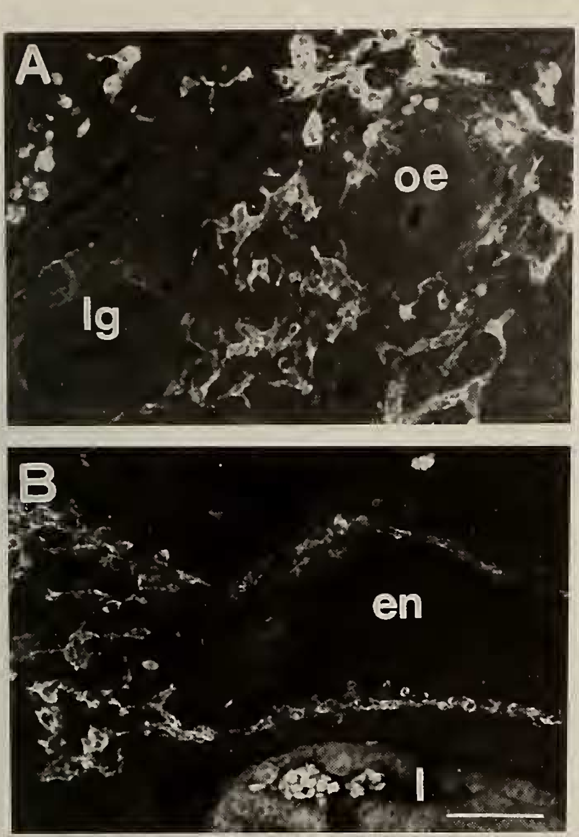

FIG. 6. HNK-1-immunoreactive creast cells distributed in the developing lung and foregut at stage 14 embryo. A, A cross section through the level of oesophagus (oe) and lung bud (lg). Crest cells are seen in the mesenchyme of the vicinity of lung bud. B, A longitudinal section through the level of foregut, the crest cells are observed between the endoderm and mesoderm of foregut. en, endoderm of the gut; 1, liver. Scale bar=100 μm.

tery at stage 12. They were found at stage 13 migrating into the lung buds. By stage 14, a number of crest cells were observed in the lung buds and foregut (Fig. 6A, B).

DISCUSSION

To our knowledge, there are only a few reports on the distribution of cranial neural crest cells in reptiles [12, 25]. The principal contribution of the present investigation was to demonstrate precise migratory routes of cranial and trunk neural crest cells in the reptilian embryo by using monoclonal antibody, HNK-1. We found that the mode of neural crest cell migration is different according to various cephalic regions and that the cranial neural crest cells seem to follow pathways similar to those of other vertebrate species studied previously [chick: 8, 26; *Xenopus*: 30; teleost: 31]. However, it has been noticed that the time of onset of cranial neural crest migration varies in non-reptile vertebrate groups [13, 14]. In mammals, Tan and Morriss-Kay [35] reported that the cranial neural crest migration already began when the neural tube is still open at neural fold stage. In birds, it has been shown that quail neural crest cells start their migration immediately before the complete closure of the neural tube [23]. On the other hand, the neural crest cell migration generally corresponds with the closure of the neural tube in amphibia [14]. In the turtle, no distinguishable neural crest cell was found when the neural tube is closed in the cephalic region. At advanced stage 8, individual neural crest cells segregated from the tube of mesencephalon and rhombencephalon, and begin their migration after aggregating once on the neural tube. Our results indicate that the cranial neural crest of the turtle has characteristic migration pattern and timing different from birds and mammals. We do not know the underlying mechanism responsible for the above-mentioned difference. Recently, however, it is increasingly accepted that the ECM (extracellular matrix) molecules may play an important role in determing the direction of neural crest cell migration and/or that ECMs provide permissive migratory substrates for their migration [28, 38]. The difference in the migratory timing of cranial neural crest cells among different vertebrate groups is likely due to the difference in environmental factors such as ECM and other unknown factors.

The migratory pathway of trunk neural crest cells has not been reported previously for reptiles. So far, the studies of the migration of trunk neural crest cells in non-reptile vertebrates have shown the following two major routes: (1) a dorsolateral pathway between the ectoderm and somite; (2) a ventral pathway between the neural tube and somite. It is noteworthy that a ventral pathway of migrating neural crest cells in somewhat different between anamniotes such as teleosts or *Xenopus* and aminotes such as birds or mammals. In birds and mammals, neural crest cell along the ventral pathway passes through the area between the anterior dermomyotome and the sclerotome [2, 11, 29]. The trunk neural crest cells in teleosts and *Xenopus* embryos migrate along the ventral pathway passing near the notochord and do not migrate into the somite [30, 31]. In our study, neural crest cells in the trunk were found to migrate along ventral pathway, which is similar to that of birds and mammals unlike that of teleosts and *Xenopus*. The difference in the antero-posterior pattern of ventral crest cell migration might be attributable to the somite tissue [4]. The ventral migrating pathway through the somite seems to be evolutionary conserved as principal character of neural crest development of amniotes. The pattern of neural crest migration along the somite is likely to be regulated by the similar nature of developmental and molecular mechanisms among reptiles and other aminotes [11].

It has been assumed that migratory pathways of neural crest cells are related to their differentiated cellular phenotypes, for example, a dorsolateral pathway is the migrating route of non-neuronal cell type including pigment cells in other vertebrate groups [fish: 31; amphibia: 27, 30; birds: 2, 20, 32; mammals: 33], whereas neural crest cells migrating along a ventral pathway will contribute to various neuronal phenotypes in the chick and mouse [20, 23, 24, 32]. We have found that, in the turtle embryos, pigment cells are located in the skin as well as in the various extracutaneous tissues such as skeletal muscle, dorsal aorta, aorta of kidney and lung [17].

Question arises as to the migration route of these extracutaneous pigment cells. The neural crest cells have been found along ventral route migrating into the myotome, on the dorsal aorta and in the lung buds. In addition, presence of some melanogenic neural crest cells located at the sites corresponding to the ventral pathway seems to indicate that pigment cells of some extracutaneous tissues are derived from neural crest cells migrating along the ventral pathway [17]. This assumption was verified by another series of experiments involving the culture of isolated somite from stage 12 embryo; the results suggest that the melanogenic crest cells along the ventral route are associated with the somite (unpublished data).

For the migration of neural crest-derived pigment cells in the trunk of the turtle embryos three possible routes can be suggested: a) They migrate along a dorsolateral pathway and give rise to pigment cells of the skin; b) they migrate along ventral pathway, while some crest cells intercalate into the myotome during midway of migration and differentiate into pigment cells of skeletal muscle; c) other precursor cells continue to migrate along ventral pathway toward the dorsal aorta and the developing kidney, where they finally differentiate into pigment cells.

It has been known that the pigment cells are not normally localized in the above-mentioned sites in the white leghorn, the quail or the mouse and that the neural crest cell migrating along a ventral pathway contributes to the dorsal root ganglia (DRG) and sympathetic ganglia (SG) [1, 20, 21]. However, the cells of DRG and SG are shown to differentiate *in vitro* into several cell types including pigment cells [6, 9, 35]. The cells of DRG and SG seem to lose the potency of differentiation into pigment cells at later stages of development [6, 9]. It is conceivable that crest cells migrating along ventral pathway are basically pluripotent in amniotes and that the loss of differentiation potency toward melanogenesis is regulated under the tissue environment in the embryo. These observations lead us to an assumption that species-specific environmental factor(s) responsible for the final differentiation of neural crest cells is present in this region.

ACKNOWLEDGMENTS

The authors thank Hattori-Nakamura Nursery of Shizuoka for providing us with the turtle eggs used in our study. This research was supported by Grant-in-aid from the Ministry of Education, Science and Culture to T. T., and Japanese Government Research Scholorship from the Ministry of Education, Science and Culture to L. H.

REFERENCES

1 Bronner ME, Cohen AM (1979) Migratory patterns of cloned neural crest melanocytes injected into host chicken embryos. Proc Natl Acad Sci USA 76: 1843–1847

2 Bronner-Fraser M (1986) Analysis of the early stages of trunk neural crest migration in avian embryos using monoclonal antibody HNK-1. Devl Biol 115: 44–55

3 Bronner-Fraser M, Fraser S (1988) Cell lineage analysis reveals multipotency of some avian neural crest cells. Nature 335: 161–164

4 Bronner-Fraser M, Stern C (1991) Effects of mesodermal tissues on avian neural crest cell migration. Devl Biol 143: 213–217

5 Chou KH, Ilyas AA, Evans JE, Quarles RH, Jungalwala FB (1985) Structure of a glycolipid reacting with monoclonal IgM in neuropathy and with HNK-1. Biochem Biophys. Res Comm 128: 383–388

6 Ciment G, Glimelius B, Nelson D, Weston JA (1986) Reversal of a developmental restriction in neural crest-derived cells of avian embryos by phorbol ester drug. Devl Biol 118: 392–398

7 Deeming DC, Ferguson MWJ (1988) Environmental regulation of sex determination in reptiles. Phil Trans R Soc Lond B 322: 19–39

8 Duband JL, Thiery JP (1982) Distribution of fibronectin in the early phase of avian cephalic neural crest cell migration. Devl Biol 93: 308–323

9 Duff RS, Langtimm CJ, Richardson MK, Sieber-Blum M (1991) *In vitro* clonal analysis of progenitor cell patterns in dorsal root and sympathetic ganglia of the quail embryo. Devl Biol 147: 451–459

10 Buncker HR (1985) The neural crest. In "Pigment Cell, Vol 7" Ed by JT Bagnara, S. Klaus, E Paul, M Schartl, Univ Tokyo Pres, Tokyo, pp 255–269

11 Erickson CA, Loring JF, Lester SM (1989) Migratory pathways of HNK-1-immunoreactive neural crest cells in the rat embryo. Devl Biol 134: 112–118

12 Ferguson MWJ (1985) Reproductive biology and embryology of the crocodilians. In "Biology of the Reptiles, Vol. 14" Ed by C Gans, F Billett, PF Maderson, John Wiley & Sons, New York, pp 329–492

13 Hall BK (1987) Tissue interaction in the development and evolution of the vertebrate head. In "Development and Evolutionary Aspects of the Neural Crest" Ed by PFA Maderson, John Wiley & Sons, New York, pp 215–259

14 Hall BK (1988) THe Neural Crest, Oxford Univ Press, London

15 Hou L (1984) Studies on the embryonic development of the turtle, *Trionyx sinensis*. Nat Sci J Hunan Normal Univ 2: 59–70

16 Hou L (1987) Cytogenesis of the primordial germ cells in the turtle, *Trionyx sinensis*. Acta Herp Sin 6: 5–10

17 Hou L, Takeüchi T (1991) Differentiation of extracutaneous melanocytes in embryos of the turtle (*Trionyx sinensis japonicus*). Pigment Cell Res 4: 158–162

18 Hou L, Takeuchi T (1992) Differentiation of reptilian neural crest cells *in vitro*. In Vitro Cell Dev Biol 28A: 348–354

19 Ito K, Takeuchi T (1984) The differentiation in vitro of the neural crest of mouse embryo. J Embryol exp Morphol 84: 49–62

20 Kitamura K, Takiguchi-Hayashi K, Sezaki M, Yamamoto H, Takeuchi T (1992) Avian neural crest cells express a melanogenic trait during early migration from the neural tube: observation with the new monoclonal antibody, "MEBL-1". Development 114: 367–378

21 Klein-Szanto A, Bradl M, Porter S, Mintz B (1991) Melanosis and associated tumors in transgenic mice. Proc Natl Acad Sci USA 88: 169–173

22 Le Douarin NM (1973) A biological cell labeling technique and its use in experimental embryology. Devl Biol 30: 217–222

23 Le Douarin NM (1982) The neural crest. Cambridge Univ

Press, Cambridge

24 Le Douarin NM (1986) Cell line segregation during peripheral nervous system ontogeny. Science 231: 1515–1522

25 Meier S, Packard DS Jr (1984) Morphogenesis of the cranial segments and distribution of neural crest in the embryos of the snapping turtle, *Chelydra serpentina*. Devl Biol 102: 309–323

26 Noden DM (1975) An analysis of the migratory behavior of avian cephalic neural crest cells. Devl Biol 42: 106–130

27 Perris R, Von Boxberg Y, Lofberg J (1988) Local embryonic matrices determine region-specific phenotypes in neural crest cells. Science 241: 86–89

28 Perris R, Bronner-Fraser M (1989) Recent advences in defining the role of the extracellular matrix in neural crest development. Comm Develop Neurobiol 1: 61–83

29 Rickmann M, Fawcett JW, Keynes RJ (1985) The migration of neural crest cells and the growth of motor axons through the rostral half of the chick somite. J Embryol exp Morphol 90: 437–455

30 Sadaghiani B, Thiebaud CH (1987) Neural crest development in the *Xenopus laevis* embryos, studies by interspecific transplantation and scanning electron microscopy. Devl Biol 124: 91–110

31 Sadaghiani B, Vielkind JR (1990) Distribution and migration pathways of HNK-1-immunoreactive neural crest cells in teleost fish embryos. Development 110: 197–209

32 Serbedzija GN, Bronner-Fraser M, Fraser SE (1989) A Vital dye analysis of the timing and pathways of avian neural crest cell migration. Development 106: 809–819

33 Serbedzija GN, Fraser SE, Bronner-Fraser M (1990) Pathways of trunk neural crest cell migration in the mouse embryos as revealed by vital dye labeling. Development 108: 605–612

34 Sieber-Blum M (1989) Commitment of neural crest cells to the sensory neuron. Science 243: 1608–1611

35 Tan SS, Morriss-Kay GM (1985) The development and distribution of the cranial neural crest in the rat embryo. Cell Tissue Res 240: 403–416

36 Vincent M, Thiery JP (1984) A cell surface marker for neural crest and placodal cells: Further evolution in peripheral and central nervous system. Devl Biol 103: 468–481

37 Weston JA (1963) An radioautographic analysis of the migration and localization of trunk neural crest cells in the chick. Devl Biol 6: 279–310

38 Weston JA (1983) Regulation of neural crest cell migration and differentiation. In “Cell Interaction and Development” Ed by KM Yamada, John Wiley & Sons, New York, pp 153–184

ZOOLOGICAL SCIENCE 11: 433–439 (1994)

© 1994 Zoological Society of Japan

The Second Maturation Division and Fertilization in the Spider *Achaearanea japonica* (Bös. *et* Str.)

Hirohumi Suzuki[1] and Akio Kondo

Department of Biology, Faculty of Science, Toho University, 2-1,
Miyama 2 chome, Funabashi-shi, Chiba 274, Japan

ABSTRACT—Formation of the main layer of the vitelline membrane, the second maturation division and fertilization were examined in the spider *Achaearanea japonica* by light and electron microscopy. Newly laid eggs had already accepted a sperm nucleus near the periphery. The sperm nucleus was observed as a mass of condensed chromatin, which was not enclosed by a nuclear envelope. Bundles of microtubules, which separated the large yolk granules that surrounded the perinuclear cytoplasm into radial arrays immediately after oviposition, seem likely to play an important role in the migration of the sperm nucleus together with perinuclear cytoplasm to the center of the egg. The matrix that was released from the vesicles, by exocytosis, into the space between the cell membrane and the outer layer of the vitelline membrane appeared to form the main layer of the vitelline membrane. The second maturation division of the first polar body progressed to telophase, but daughter nuclei were not formed. The maturation division of the secondary oocyte was strictly synchronized with respect to that of first polar body, and it generated the female pronucleus and the nucleus of the second polar body. The female pronucleus moved toward the egg's center, in which the male pronucleus was now located, for conjugation. The larger pronucleus was probably the male pronucleus, and the other one was probably the female pronucleus.

INTRODUCTION

Embryos of many spiders have been examined in detail under the light microscope. However, very little information is available about the maturation and fertilization of the egg. We have previously examined the fine-structural changes at the egg's surface during the first maturation division in the spider *Achaearanea japonica* (unpublished data). The cell membrane begins to invaginate from the egg's surface, and then the lumen of each invagination becomes wider, forcing the large yolk granules into outer radial columns and an inner spherical mass (see Fig. 5). The matrix that is discharged at the egg's surface by secretion granules appears to form the outer layer of the vitelline membrane. In this report, we describe the formation of the main layer of the vitelline membrane, the second maturation division and fertilization in *A. japonica*.

MATERIALS AND METHODS

Mature females of *Achaearanea japonica* (Bös. *et* Str.) lay eggs 5–6 times in mid- and late summer, and about 100 eggs are released at each oviposition. The eggs are spherical and 0.5 mm in diameter. Eggs collected on the campus of Toho University were used for the present study. They were incubated at 25°C.

Routine light microscopy was carried out using paraffin-embedded serial sections. Eggs fixed in FAA (formalin, ethyl alcohol and acetic acid, 5:15:1, v/v) were dehydrated in a graded alcohol series, cleared in toluene and embedded in paraffin. The samples were cut off by 30 μm with a microtome, left in distilled water for 3 days and then sectioned at 6- to 8-μm thickness. For more detailed light-microscopic observations, eggs were fixed for the most part in a mixture of 2.5% glutaraldehyde and 2% paraformaldehyde in 0.1 M phosphate buffer, pH 7.4, that contained 0.2 M sucrose, and they were punctured during fixation with a tungsten needle. Dehydrated samples were embedded in methacrylate resin Technovit 7100 (Kulzer). The resin-embedded specimens were sectioned at 1- to 5-μm thickness with a glass knife on a LKB-4800 ultramicrotome. The sections were stained with Mayer's acid-haemalum and eosin.

For fine-structural observations, the eggs were prefixed, at room temperature, for 3 hr in a mixture of 2% paraformaldehyde and 2.5% glutaraldehyde in 0.1 M phosphate buffer, pH 7.4, that contained 0.2 M sucrose. During fixation, the eggs were cut in half with a tungsten needle. After rinsing for more than one hour with the same buffer plus 0.2 M sucrose, the samples were postfixed, at room temperature, for one hour in 2% osmic acid in 0.1 M phosphate buffer, pH 7.4, without sucrose. After rinsing with the same buffer without sucrose, samples were dehydrated in a graded alcohol series, transferred to propylene oxide, and embedded in epoxy resin Quetol 812 (Nisshin EM). Ultrathin sections were cut with a diamond knife on the ultramicrotome, stained with uranyl acetate and lead citrate, and examined under a JEOL JEM-1210 or a Hitachi HU-12A electron microscope. Thick sections were prepared simultaneously, and these sections were stained with toluidine blue for light microscopy. They were reembedded in the same epoxy resin for electron microscopy as needed.

RESULTS

Just at the time when oviposition occurred, the eggs had already accepted a sperm nucleus near the periphery, about 50 μm from the egg's surface (Fig. 1). No spermatozoa were observed at all. The cytoplasm was distributed at the egg's surface as periplasm, 10–20 μm in thickness, and in the

Accepted June 6, 1994
Received March 28, 1994

---

[1] To whom correspondence should be addressed.

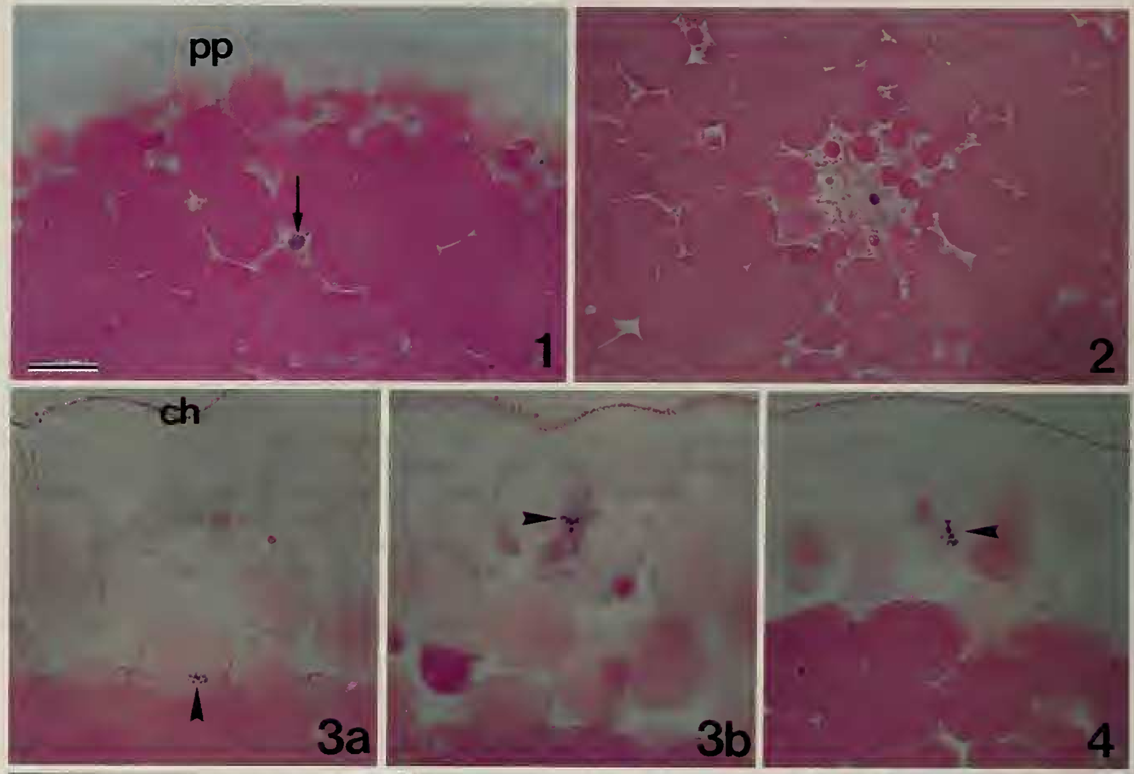

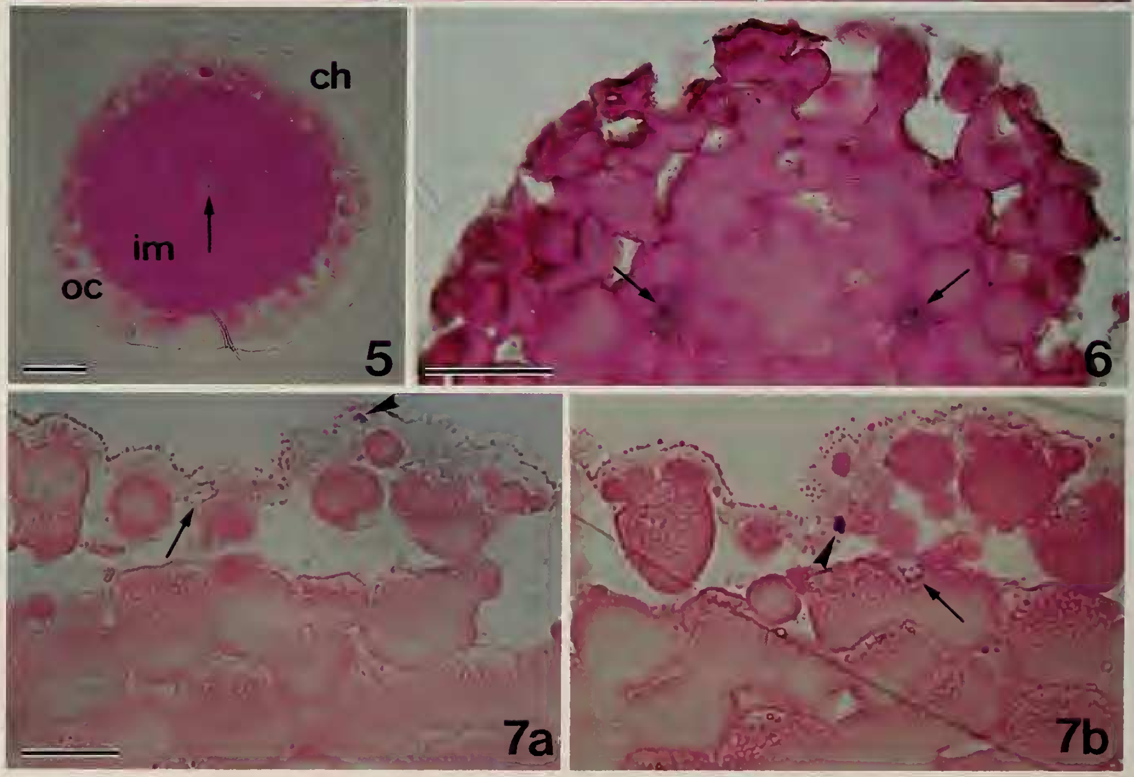

Figs. 1–4. Technovit-embedded sections. Scale bar = 20 μm. Fig. 1. Just at the time of oviposition. The egg has already accepted a sperm nucleus (arrow). The cytoplasm is distributed at the egg's surface as periplasm (pp) and in the perinuclear zone. Fig. 2. Twenty minutes after oviposition. The large yolk granules surrounding the perinuclear cytoplasm of the sperm nucleus are organized in radial arrays. Fig. 3a. Forty-five minutes after oviposition. The large yolk granules are arranged in outer radial columns and an inner spherical mass (compare with Fig. 5). The maturation division of the secondary oocyte at metaphase (arrowhead) is seen at the surface of the inner spherical yolk mass. The equatorial plane is perpendicular to the egg's surface. ch, chorion. Fig. 3b. Same egg as in Fig. 3a. The second maturation division of the first polar body at metaphase (arrowhead) is seen in the cytoplasm located among the outer radial columns of yolk granules. The equatorial plane is parallel to the egg's surface. Fig. 4. A different egg, 45 min after oviposition. The first polar body at metaphase during the second maturation division (arrowhead) is seen in the periplasm. The equatorial plane is perpendicular to the egg's surface.

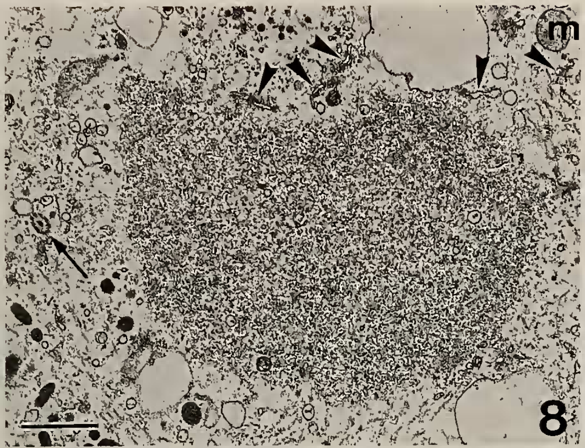

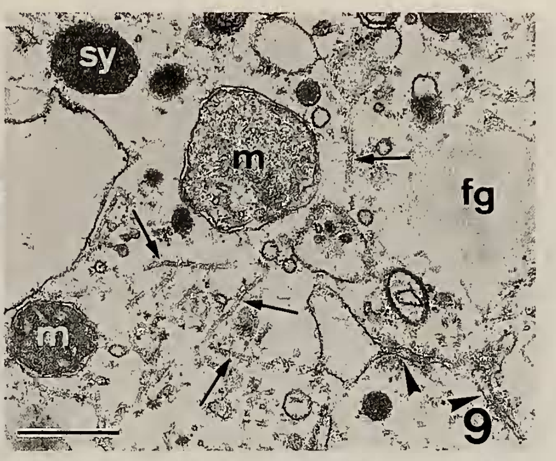

FIG. 8. Electron micrograph showing the sperm nucleus. The sperm nucleus is seen as a mass of electron-dense chromatin without a nuclear envelope. A cross section of axial filament of the spermatozoon (arrow) and fragments of the nuclear envelope (arrowheads) are visible in the perinuclear cytoplasm. Scale bar=1 μm. m, mitochondrion with a weakly electron-dense matrix.

FIG. 9. The perinuclear cytoplasm of the sperm nucleus. Microtubules are scattered around (arrows). Mitochondrion with a highly electron-dense matrix (m, white lettering) and that with a weakly electron-dense matrix (m, black lettering) are visible. Scale bar=0.5 μm. arrowheads, fragments of the nuclear envelope; fg, fatty granule; sy, small yolk granule.

perinuclear zone around the sperm nucleus. The first maturation division of the oocyte, which was in the telophase, was visible in the periplasm (data not shown). The sperm nucleus, about 5 μm in diameter, migrated toward the center of the egg as development proceeded. It was clear that this nucleus was not cleavage nucleus. Under the electron microscope, the sperm nucleus was observed as a mass of electron-dense chromatin (Fig. 8). A complete nuclear envelope was not observed but fragments of nuclear envelope were observed in the perinuclear cytoplasm (Fig. 8 and 9). Axial filament of the spermatozoon was observed near the nucleus (Fig. 8). Microtubules were scattered about (Fig. 9). Mitochondria were spherical or oval with faintly developed cristae. Some of them had a highly electron-dense matrix but others had a weakly electron-dense matrix (Fig. 9). The large yolk granules surrounding the perinuclear cytoplasm were organized in radial arrays from 20 min after oviposition (Fig. 2).

Thirty minutes after oviposition, the bursting of vesicles was observed at the surface of the egg, and the matrix of the vesicles was scattered in the space between the cell membrane and the outer layer of the vitelline membrane (Fig. 10). Mucous material and fibrils, which were of the same electron density as the matrix of the vesicles, began to accumulate under the outer layer of the vitelline membrane. Microvilli protruded from the cell membrane. The eggs were difficult to dechorion from this stage.

Forty-five minutes after oviposition, two chromosome plates at metaphase, one being that of the secondary oocyte and the other being that of the first polar body, were observed. The second maturation division of the secondary oocyte occurred at the surface of the inner spherical yolk mass, and its equatorial plane was perpendicular to the egg's surface (Fig. 3a). A total of 15 eggs was employed for examination of the second maturation division of the first polar body. The spindle was situated at the periplasm in 9 eggs, while in the other 6 eggs it was observed at the cytoplasm somewhere among the outer radial yolk columns. In the former case, the equatorial plane was located perpendicularly to the egg's surface (Fig. 4), by contrast, in the latter case it was parallel to the egg's surface (Fig. 3b). Electron micrographs of maturation divisions could not be obtained because of failure in the staining of thick, epoxy-resin-embedded sections.

One hour after oviposition, the sperm nucleus arrived at the center of the egg (Fig. 5). Until this stage, in a few eggs, several nuclei resembling the sperm nucleus were observed (Fig. 6). The number of such nuclei per egg was usually two or three, while the maximum number was seven, in the present investigation. They were considered to be the result of polyspermy.

Ninety minutes after oviposition, the vitelline membrane

FIG. 5. One hour after oviposition. Technovit-embedded section. The large yolk granules are arranged in outer radial columns (oc) and an inner spherical mass (im). The sperm nucleus, accompanied by perinuclear cytoplasm, is seen at the center of the egg (arrow). The large yolk granules surrounding the perinuclear cytoplasm are organized as radial arrays. Scale bar=100 μm. ch, chorion.

FIG. 6. One hour after oviposition. Paraffin-embedded section. Two sperm nuclei, a result of polyspermy, are visible in the egg (arrows). Scale bar=50 μm.

FIG. 7. One hour and thirty minutes after oviposition. Technovit-embedded sections of an egg. Scale bar=20 μm. Fig. 7a. The nucleus of the second polar body (arrow) and one chromosomal mass after the second maturation division of first polar body (arrowhead) are seen in the periplasm. Fig. 7b. Another chromosomal mass, generated by the division of the first polar body, (arrowhead) is seen in the periplasm, and the female pronucleus (arrow) is seen at the surface of the inner spherical yolk mass.